nature cell biology

Transient colocalization of X-inactivation centres accompanies the initiation of X inactivation

Christian P. Bacher[1], Michèle Guggiari[2], Benedikt Brors[1], Sandrine Augui[2], Philippe Clerc[3], Philip Avner[3], Roland Eils[1,4,5,6] and Edith Heard[2,5,6]

The initial differential treatment of the two X chromosomes during X-chromosome inactivation is controlled by the X-inactivation centre (*Xic*). This locus determines how many X chromosomes are present in a cell ('counting') and which X chromosome will be inactivated in female cells ('choice'). Critical control sequences in the *Xic* include the non-coding RNAs *Xist* and *Tsix*, and long-range chromatin elements. However, little is known about the process that ensures that X inactivation is triggered appropriately when more than one *Xic* is present in a cell. Using three-dimensional fluorescence *in situ* hybridization (FISH) analysis, we showed that the two *Xic*s transiently colocalize, just before X inactivation, in differentiating female embryonic stem cells. Using *Xic* transgenes capable of imprinted but not random X inactivation, and *Xic* deletions that disrupt random X inactivation, we demonstrated that *Xic* colocalization is linked to *Xic* function in random X inactivation. Both long-range sequences and the *Tsix* element, which generates the antisense transcript to *Xist*, are required for the transient interaction of *Xic*s. We propose that transient colocalization of *Xic*s may be necessary for a cell to determine *Xic* number and to ensure the correct initiation of X inactivation.

Mammalian X chromosome inactivation involves the differential treatment of two identical chromosomes within the same nucleoplasm. The initial target of this differential treatment is the *Xic*. For X inactivation to occur, cells must register the presence of at least two *Xic*s[1,2]. Only a single X chromosome remains active in a diploid cell; all extra X chromosomes are inactivated. Inactivation is triggered by accumulation of the *Xist* transcript (the gene is located in the *Xic* region), which coats and inactivates chromatin *in cis*. The mechanisms underlying recognition of the number of *Xic*s and the differential treatment of the two *Xic*s have yet to be described. The product of antisense transcription of *Xist* (*Tsix*) and *cis*-regulatory sequences are involved in the choice and counting functions of the *Xic* (for reviews see refs 3, 4). Deletion of the 65-kb region located 3′ of *Xist* affects choice, leading to non-random inactivation of the chromosome carrying the deleted allele[5]. The 65-kilo base (kb) deletion also affects counting, as X inactivation is triggered even in cells with only one X chromosome[5]. Further delineation of this region has been achieved using a Cre–lox mediated DNA re-insertion strategy[6], but little is known about the actual mechanisms that mediate counting and choice. Furthermore, although the 3′ region of *Xist* is clearly important for correct random X inactivation, transgenic studies have shown that the *Xic* sequences tested to date may not be sufficient for *Xic* function and/or recognition. Large single-copy *Xist* transgenes cannot trigger *cis*-inactivation or inactivation of the endogenous X chromosome during embryonic stem cell differentiation[7], despite containing the counting and choice elements 3′ of *Xist*. These transgenes may not be recognised by cells as ectopic *Xics* when present as a single-copy insertion. A possible explanation may be that the *Xic*s have to associate with a nuclear compartment, and/or transiently interact with each other, to exchange information and to coordinate the subsequent random X-inactivation process[7,8]. Nuclear mis-localization may thus prevent a single-copy transgene from being 'sensed' as an additional *Xic* and this would mean that X inactivation is not triggered. Interactions between unlinked, but coordinately regulated chromosomal loci, or colocalization of genes within specific nuclear compartments, may be important for gene regulation[9–13]. In the case of X inactivation, nuclear compartmentalization was one of the earliest models proposed to explain the differential treatment of the two X chromosomes in the same nucleus[14].

We set out to examine whether the *Xic* locus shows any signs of non-random spatial distribution in the nucleus that may reflect, or underlie, its specific functions in controlling X inactivation. Several embryonic stem cell lines, at various stages of *in vitro* differentiation were examined (Table 1 and see Supplementary Information, Fig. S1). Two-dimensional analysis of differentiating female embryonic stem cells using DNA FISH to simultaneously detect the *Xic* and the X chromosome, or RNA FISH to detect *Xist* transcription, suggested that the two *Xic*s come into very close proximity during the initiation of X inactivation (Fig. 1a, b). To assess this observation more accurately, three-dimensional FISH and

[1]German Cancer Research Center (DKFZ), Im Neuenheimer Feld 280, D-69120 Heidelberg, German. [2]CNRS UMR 218, Curie Institute, 26 rue d'Ulm, 75248 Paris Cedex 05, France. [3]Pasteur Institute, 25 rue du Docteur Roux, Paris 75015, France. [4]Institute of Pharmacy and Molecular Biotechnology (IPMB), University of Heidelberg, Im Neuenheimer Feld 364, 69120 Heidelberg, Germany. [5]These authors contributed equally to this work.
[6]Correspondence should be addressed to E.H. or R.E. (e-mail: Edith.Heard@curie.fr; r.eils@dkfz-heidelberg.de)

Received 31 October 2005; accepted 11 January 2006; published online; 24 January 2006; DOI: 10.1038/ncb1365

Table 1 Embryonic stem cell lines

Cell line	Genotype	Counting and choice	*Tsix* transcription	*Cis* inactivation	Reference or source
HM1	XY	Yes	Yes	NA	Gift from E. Wagner
CK35	XY	Yes	Yes	NA	Ref. 7
PGK1 (PGK12.1)	XX	Yes	Yes	Yes	Ref. 27
HP310	XX	Yes	Yes	Yes	Ref. 5
D102	$XX^{\Delta 65kb}$	No	No*	Yes	Ref. 5
c.16.1	$XX^{\Delta 65kb+16kb}$	No	Yes	Yes	Ref. 16
53BL	$XY+Xic^{Tgn=1}$	No	Yes	No	Ref. 7
L412	$XY+Xic^{Tgn>1}$	Yes	Yes	Yes	Ref. 7

NA, not applicable. *No *Tsix* transcription on the deleted ($XX^{\Delta 65kb}$) allele only.

tailored image analysis were performed (Fig. 1 and see Supplementary Information, Fig. S2) on female embryonic stem cells (PGK and HP310, see Table 1) and mouse embryonic fibroblasts (MEFs). The *Xic* loci were detected using DNA FISH, and the X chromosome undergoing inactivation was identified using *Xist* RNA FISH. Close proximity of the two *Xic* loci (within an interval of 0–1 μm) was detected in a fraction (8–15%) of both female embryonic stem cell lines, at days 1.5–2 of differentiation (Fig. 2). Male embryonic stem cells containing multicopy yeast artificial chromosome (YAC) *Xic* transgenes (L412, Table 1) that were previously shown to induce *cis*-inactivation and counting[7] also showed colocalization between the endogenous *Xic* and the transgenic locus (Fig. 2). In MEFs, where X inactivation is fully established, and in undifferentiated embryonic stem cells with two active X chromosomes, close proximity of *Xic*s was shown in <3% of cells, which corresponds to background fluctuations[9]. The significance of the *Xic*–*Xic* proximity detectable only during early embryonic stem cell differentiation was confirmed using quantile-quantile plot analysis. This was performed by running each data set against the MEF distribution (data not shown) or against a random point population of simulated points in a virtual cell (Fig. 3, see Methods). A shift to shorter than expected inter-*Xic* distances was found for PGK, HP310 and L412 embryonic stem cell lines, particularly at 1.5–2 days of differentiation, whereas no such shift was observed for the female MEF control (Fig. 3). FISH analysis also revealed that the *Xic* locus tends to occupy a very peripheral position in the nucleus in all cell lines tested (see Supplementary Information, Fig. S3). Furthermore, for the majority of *Xic* colocalization events (inter-*Xic* distances of < 1μm), the distance of each of the two *Xic*s from the nuclear envelope was found to be within a range of 0.1–0.8 μm (data not shown), indicating that *Xic*–*Xic* colocalisation tends to occur close to the periphery.

We next examined when exactly *Xic*–*Xic* colocalization occurs relative to *Xist* RNA accumulation. In the majority (>90%) of nuclei, where the *Xic*–*Xic* distance was <1 μm, *Xist* RNA had not yet accumulated (see Supplementary Information, Fig. S4). Therefore, *Xic* colocalization precedes accumulation of *Xist* RNA on one of the two X chromosomes, suggesting that colocalization may be linked to the initiation of X inactivation. To assess the functional significance of *Xic*-*Xic* colocalization, embryonic stem cell lines that are defective in *Xic* function were analysed. A male cell line, 53Bl, carrying a single copy *Xic*YAC transgene that includes *Xist* and130 kb of upstream and 310 kb of downstream sequence, integrated at chromosome 13 was examined. Single-copy *Xist* transgenes are incapable of inducing random X inactivation (either *cis*-inactivation or inactivation of the endogenous X) during embryonic stem cell differentiation[7], although they can efficiently induce imprinted X inactivation[15]. During the induction of imprinted X inactivation, however, the counting and choice functions of *Xic* are not normally used, as they are over-ridden by a parent-specific imprint on *Xist*. We postulated that the lack of function of these single-copy transgenes during random X inactivation may be linked to their incapacity to be registered by the cell as a second *Xic*. The expected distance distribution relative to the nuclear periphery was observed for both the transgenic and endogenous *Xic*s (data not shown). However, when inter-*Xic* distances were measured in 53Bl cells during differentiation, a marked absence of colocalization between the two *Xic* signals was observed (Fig. 2). Quantile–quantile plot analysis revealed that inter-*Xic* distances for the 53Bl line were similar to a random simulation (Fig. 3a). However, a significant shift from the inter-*Xic* distance distributions seen for female embryonic stem cell lines was found (Fig. 3b). The complete absence of *Xic* colocalization in the 53Bl line correlates with the inability of this transgene to induce counting, choice and *cis*-inactivation during embryonic stem cell differentiation.

To investigate the nature of the link between *Xic* colocalization and X inactivation further, a female embryonic stem cell line (D102, derived from the HP310 line[5]; see Table 1), carrying a 65-kb deletion within one of the two *Xic*s, was analysed . In D102 cells, X inactivation is no longer random, as the deleted $X^{\Delta 65kb}$ chromosome is always chosen for inactivation on differentiation. The *Xic* counting function the $X^{\Delta 65kb}$ chromosome is also disrupted, as in $X^{\Delta 65kb}O$ or $X^{\Delta 65kb}Y$ embryonic stem cells (containing only one X chromosome), the $X^{\Delta 65kb}$ chromosome undergoes inactivation on differentiation[6], unlike wild type XO or XY cells, where X inactivation is never observed. Strikingly, no *Xic* colocalizations (that is, distances between 0–1 μm) were observed at any stage of differentiation in this cell line (Fig. 2). Quantile–quantile plot analysis confirmed the difference in distributions of inter-*Xic* distances between D102 and HP310 cells (Fig. 3). In fact, the *Xic* loci in D102 cells seem to be even further away from each other than expected. The 65-kb region 3′ of *Xist* (which includes counting elements, and the promoter and 5′ end of *Tsix*) must therefore be important for the *Xic* interactions observed in female embryonic stem cells. To define which part of this region may be important for *Xic* colocalization, the c.16.1 cell line derived from D102 (Table 1) was analysed. In this line, 16 kb of sequence 3′ of *Xist* (up to and including the *Tsix* promoter) was reinserted using Cre–lox-mediated targeting[16]. *Tsix* transcription is reconstituted in c.16.1 cells, although X inactivation remains non-random, with only the targeted allele being inactivated[16]. When inter-*Xic* distances were measured, *Xic*–*Xic* colocalization was found to be completely re-established in this cell line, at days 1.5 and 2 of differentiation, with frequencies comparable to HP310 (the original parental line of D102; Fig. 2). Thus, we concluded that the incapacity of the D102 line to show close *Xic*–*Xic* proximity during differentiation was due to the absence of the

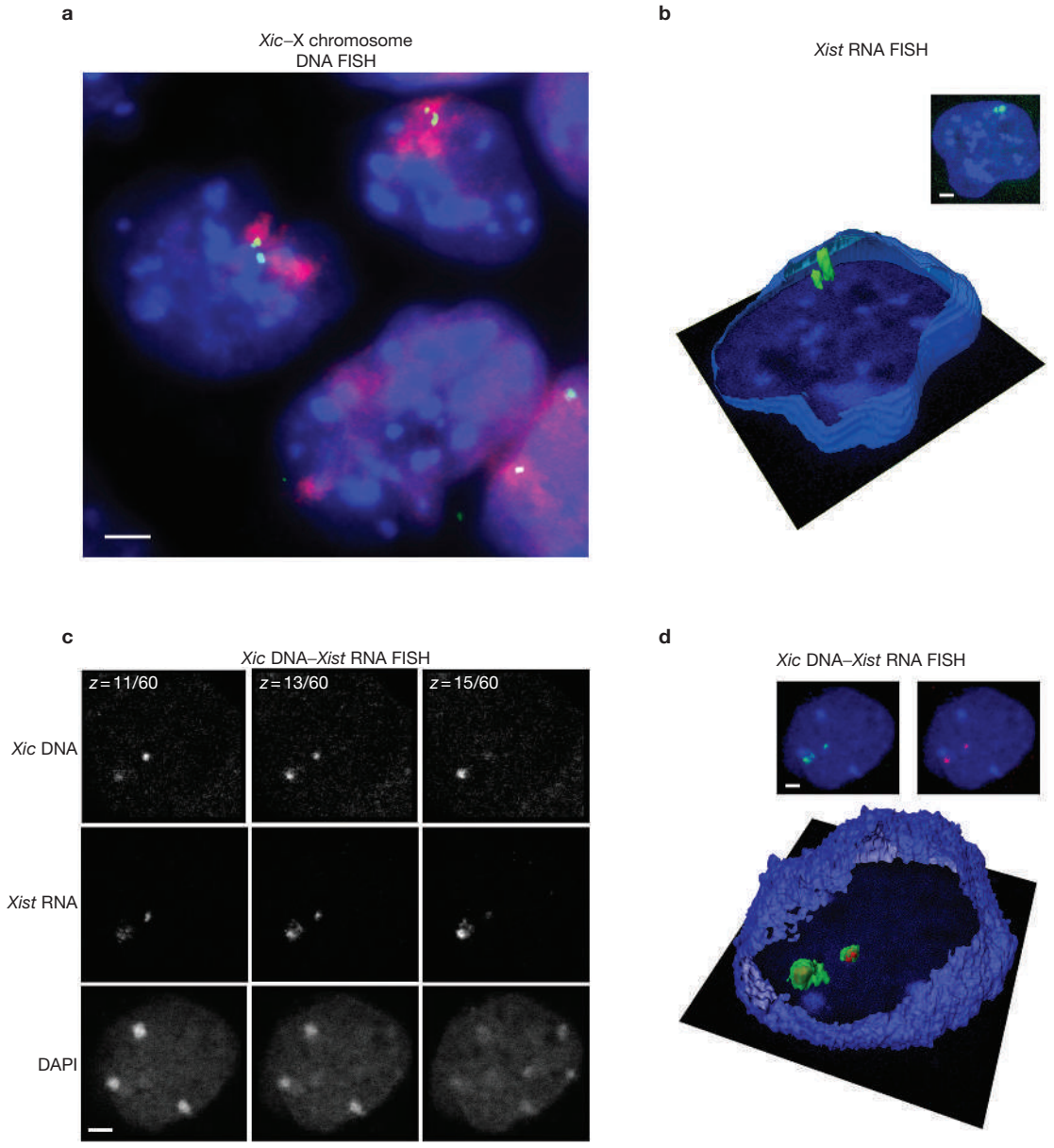

Figure 1 Nuclear location of the *Xic* and *Xist* RNA in differentiating embryonic stem cells. (**a**) Female embryonic stem cells differentiated for 2 days were analysed by DNA FISH using an X-chromosome paint (red) and an *Xic* probe (green). Nuclei were counterstained with DAPI (blue). (**b**) *Xic* colocalization in female embryonic stem cells at day 1.5 after differentiation. The insert shows a three-dimensional projection of the original DAPI DNA counterstained image with *Xist* RNA signals (green). (**c**) Raw data obtained by confocal microscopy on female embryonic stem cells following *Xist* RNA–*Xic* DNA FISH. Three of of the 60 sections acquired for this nucleus are shown. The distance between these sections along the *z* axis was approximately 0.4 μm. (**d**) Before visualization, DAPI-stained nuclei were pre-processed and segmented to allow isosurface extraction (see Supplementary Information, Fig. S2). The nuclei were cut open to visualize the *Xist*–*Xic* signals (green and red, respectively). The insert shows a three-dimensional projection of original DAPI DNA counterstained images overlaid by the *Xist* RNA signal and *Xic* DNA signal (red; lower right only), respectively. Scale bars represent 2 μm.

16-kb region immediately 3′ of *Xist* and that the *Tsix* transcription unit was necessary for colocalization to occur. The observation that although *Xic* colocalization is reconstituted, X inactivation remains non-random in this cell line, suggests that colocalization of *Xic*s may be necessary, but is not sufficient, for counting and choice.

Using high-throughput three-dimensional FISH and large-scale image analysis, we have demonstrated that the two *Xic*s transiently come into close proximity during the initiation of random X inactivation. Colocalization may involve either a direct physical interaction, or alternatively positioning within a common nuclear sub-compartment. Its function may be to allow a cell to sense that more than one *Xic* is present in a cell and to ensure that random X inactivation occurs. This sensing step is likely to be an upstream event in the X-inactivation initiation process, as it occurs just before *Xist* RNA accumulation. Taken together, our analysis of *Xic* transgenes and deletions suggests that although it is not sufficient (c.16.1 cells), colocalization is likely to be necessary (53BL cells) for correct counting and choice to occur. It is not currently known whether *Xic* colocalization is dependent on autosomal ploidy, as counting is[3,4]. We have demonstrated that colocalization between *Xic*s requires long-range sequences that are absent

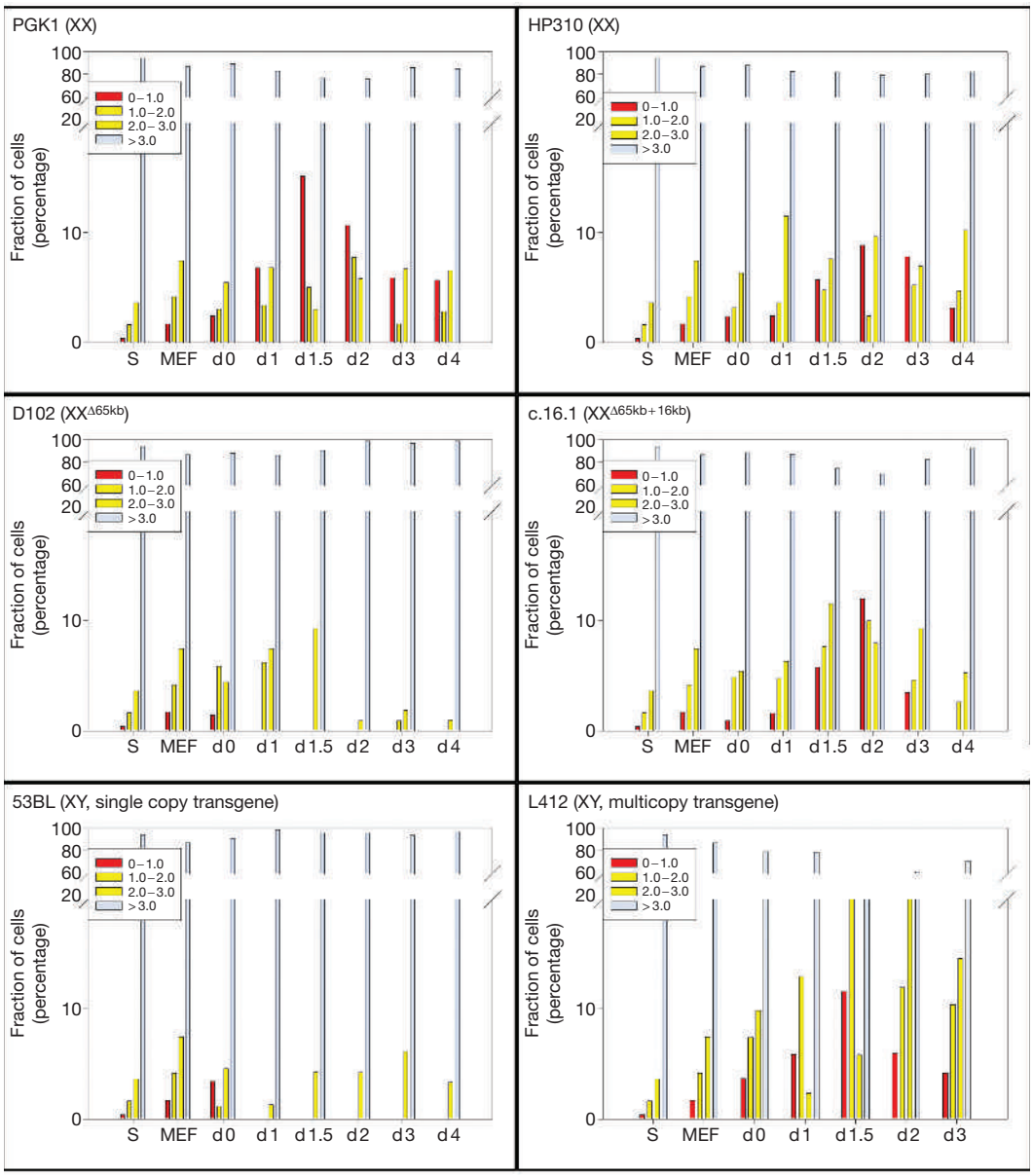

Figure 2 *Xic* colocalization in differentiating embryonic stem cells. *Xic* colocalization (or cross talk) events were detected in wildtype female (PGK1, HP310), female counting-deficient (D102, c.16.1), and transgenic male (53BL, L412) embryonic stem cells. A striking increase in *Xic* crosstalk events was observed for PGK1, HP310 and L412cell lines at days 1.5 and 2.0 after induction of X-chromosome inactivation. A general decrease in crosstalk events and an absence of *Xic* approximation events within the distance range of 0–1 μm was observed in 53Bl and D102 cells. S, simulated distribution of 1,000 calculated *Xic* distances from a random and uniform distribution within a simulated cell nucleus; MEF, control experiment using male or female MEF populations; d, days after the start of differentiation.

from a 460-kb *Xic* transgene, although their absence can be compensated for in a multi-copy array of this transgene. Thus, at least part of the region required for crosstalk must be present in the 460-kb sequence. We have also shown that the presence of the region immediately 3′ of *Xist* , including the *Tsix* promoter, is required for colocalization to occur. *Tsix* transcription may be important for this process, either at the RNA or chromatin level[17–19]. However, it cannot be sufficient, as in undifferentiated female embryonic stem cells, *Tsix* is transcribed and yet there is no significant *Xic* colocalization.

The transient *Xic* colocalization we have observed within a restricted developmental time window seems to be specific to this region of the X chromosome and to its particular functions in random X inactivation for several reasons: First, *Xic* multi-copy transgenes on autosomes also display *Xic* colocalization; second, the 65-kb deletion 3′ of *Xist* abolishes this *Xic* colocalization, suggesting *Xic* specificity rather than an X-chromosome wide phenomenon; third, other genomic loci that have been examined to date do not show this type of colocalization (data not shown). Furthermore, our preliminary data suggests that the imprinted *Snrpn* gene, previously found to show transient homologous associations during late S phase in T cells[20], shows no homologous association in embryonic stem cells at 1.5 days of differentiation (S. A., M. G. and E. H., unpublished observations). However, imprinted loci may have no reason to transiently interact during embryonic stem cell differentiation, as their mono-allelic expression patterns are established before this stage

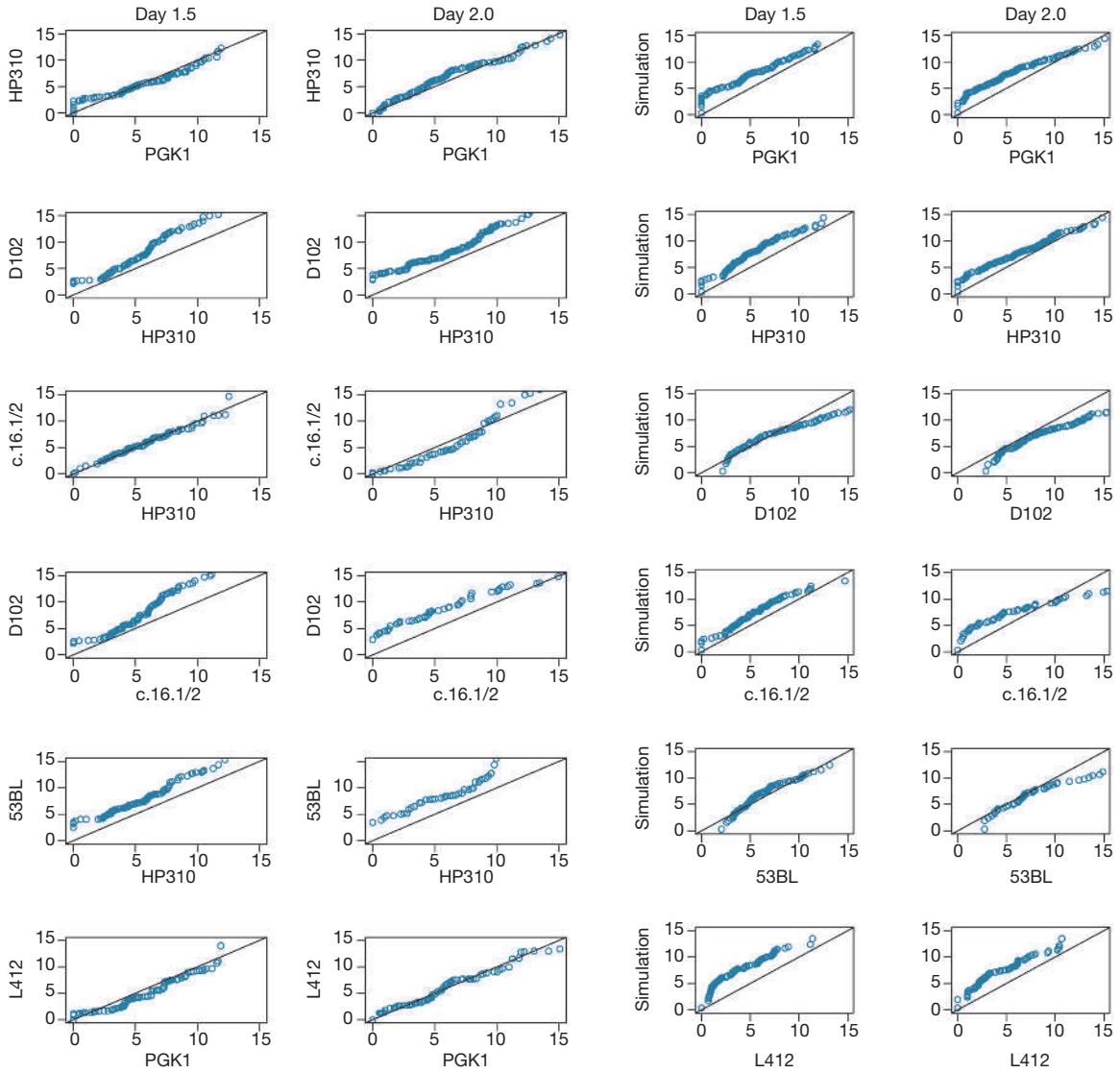

Figure 3 Analysis of inter-*Xic* distance distributions using quantile–quantile plots. **(a)** Visualization of the *Xic* distance distributions using quantile–quantile plots for the indicated embryonic stem cell lines analysed (at days 1.5 and 2 of differentiation) against a simulation of 1,000 randomly determined *Xic* distance distributions. Closer than expected proximity between the two *Xic*'s was observed in PGK, HP310 and c.16.1 cell lines (indicated by a shift of the points above the 45° reference line), whereas a complete lack of the short *Xic* inter-distance population was observed in the 53BL and D102 cell lines (indicated by a shift of the points below the 45° reference line). (**b**) Comparison of wild type XX embryonic stem cell lines (HP310 and PGK) against the transgenic 53Bl (single copy) and L412 (multicopy) cell lines, and the deleted D102 and c.16.1 cell lines, at days 1.5 and 2 of differentiation. The quantile–quantile plots of PGK against HP310 distributions, for each day, lay approximately along the 45° reference line, and thus indicated that they have similar distributions. The slight shift towards shorter inter-*Xic* distances for PGK cells at day 1.5 after induction of differentiation was explained by the slightly slower inactivation kinetics observed for HP310 cells. The L412 line showed a very similar distribution to the other female lines. A lack of any close proximity between the two *Xic* loci was observed in 53BL and D102 cells when compared with wild-type PGK and HP310 cells. The complemented c.16.1 cells showed no shift when compared to the female HP310 cell lines, indicating that close proximity of the *Xic*s was restored in this line.

of development. In this context, *trans*-interaction of *Xics* is also unlikely to be necessary for imprinted paternal X inactivation, where counting and choice functions are not initially required, given the presence of a germ line imprint repressing the maternal *Xist* gene. The capacity of single-copy transgenes to induce imprinted[15], but not random X inactivation[7] supports this assertion.

Our findings underline the potential importance of *trans*-interactions for mono-allelic gene regulation, which in the case of X inactivation, has an impact on gene expression on a chromosome-wide scale. The exact nature and duration of the interaction between the two *Xic*s in living cells has yet to be examined. Given the recent evidence that co-ordinately regulated genes on non-homologous chromosomes can become juxtaposed in mammalian cells[9,10], it will be important to define how widespread homologous locus interactions are in mammals and whether they correlate with random, mono-allelic expression patterns. □

METHODS

Cell lines and cell culture. Female mouse embryonic fibroblasts, prepared from 13.5 d embryos were cultured in DMEM with GlutMAX (GIBCO–Invitrogen, Cergy Pontoise, France) supplemented with 10% fetal bovine serum (FBS; GIBCO–Invitrogen). Male and female embryonic stem cell lines were grown either on monolayers of mitomycinc C-treated feeder cells (HP310, D102, c.16.1, 53Bl and L412) as previously described[5,7]; or on gelatin-coated flasks or plates

(feeder-free PGK12.1 and HM1) as previously described[21]. Embryonic stem cells were maintained in an undifferentiated state in DMEM with GlutMAX, 15% fetal calf serum (GIBCO), 0.1 μM 2-mercaptoethanol (Sigma, St Louis, MO), and 1000 U ml^{-1} leukaemia inhibitory factor (LIF). Differentiation of embryonic stem cells was induced by pre-adsorbing feeders (in the case of feeder-dependent embryonic stem cell lines[7]), removing LIF and using 100 nM all-trans-retinoic acid (RA, Sigma) in DMEM supplemented with 10% FBS, and 0.1 μM 2-mercaptoethanol. Differentiation medium was changed daily. All cells were grown at 37 °C in 8% CO_2. Feeder-free male HM1 cells were a gift from E. Wagner; feeder-free female PGK12.1 cells were a gift from N. Brockdorff.

RNA and DNA FISH. Fibroblasts or embryonic stem cells cultured on gelatin-coated coverslips were fixed in 3% paraformaldehyde for 15 min at room temperature. Permeabilization of the cells was performed on ice in PBS containing 0.5% Triton X-100, and 2mM vanadyl ribonucleoside complex (New England Biolabs, Ispswich, MA) for 3.5 min. The coverslips were rinsed twice and kept in 70% ethanol. Before FISH, the coverslips were dehydrated through an ethanol series (70%, 90%, 100%), air-dried and then rehydrated in 2× SSC. The DNA was then denatured in 50% formamide, 2× SSC for 40 min at 80 °C in an oven. The coverslips were then placed in ice cold 2× SSC, rinsed once and simultaneous RNA–DNA FISH was performed. The *Xist* probe used was a 19-kb genomic fragment derived from a lambda clone (510) that covers most of the *Xist* gene[7]. The *Xic* probe (YAC PA-2) has previously been described[7]. Probes were labelled by nick translation (Abbott–Vysis, Rungis, France) with spectrum green or red-dUTP (Vysis). Hybridization used 0.1 μg of probe (per coverslip) precipitated with 10 μg of salmon sperm and resuspended in 50% formamide, 2× SSC, 20% dextran sulfate, 1 mg ml^{-1} BSA (New England Biolabs), 200 mM vanadyl ribonucleoside complex (VRC), overnight at 37 °C. After three washes in 50% formamide with 2× SSC and three washes in 2× SSC at 42 °C, DNA was counterstained for 2 min in 0.2 mg ml^{-1} DAPI, followed by a final wash in 2× SSC. Samples were mounted in 90% glycerol, 0.1× PBS, 0.1% p-phenylenediamine at pH 9 (Sigma).

Confocal microscopy. Fixed cell imaging was carried out on a confocal laser scanning microscope TCS SP2 AOBS (Leica Microsystems, Wetzlar, Germany) using a × 63 oil immersion objective with 1.4 optical apperture (HCX PL APO lbd.BL x 63/1.4, #506192, Leica Microsystems). A diode laser (λ = 405 nm) was used for excitation of DAPI counterstain. An argon (λ = 488 nm) and a helium–neon laser (λ = 543 nm) were used for spectrum green (*Xist* RNA) probe and spectrum red (*Xic* DNA probe) excitation, respectively. Three-dimensional image stacks with an image format of 1024 × 1024 pixel and constant voxel sizes of 0.058 μm × 0.058 μm × 0.204 μm were acquired. The number of *z*-stacks was adjusted according to the heights of the cell nuclei resulting in an average amount of 40 two-dimensional images for each cell nucleus. The DAPI stained chromatin, *Xist* probes and *Xic*-DNA probes were acquired in parallel at constant scanning speed of 800 Hz. The laser intensities were adjusted to an optimal signal-to-noise ratio and kept constant for all imaged slides. For this purpose the acousto-optical beam splitters were set to 35% for the diode laser and to 40% for the argon and helium–neon laser. The photo multiplier settings where adjusted to 499.7 volts for the diode laser, 650.3 volts for the argon and 628.6 volts for the helium–neon lasers.

Segmentation of cell nuclei. Image processing was carried out using our in-house developed image analysis platform, TIKAL[22], running on a high-performance computing cluster. Segmentation of cell nuclei was performed automatically. Segmentation results were checked manually and confirmed for each individual cell nucleus. This manual step was necessary to identify and avoid false segmentation due to hybridization artifacts and to eliminate oversegmented cells. Oversegmentation was a result of the tendency of embryonic stem cells to grow in closed colonies and the insufficient resolution of the microscope to resolve the nuclear borders at a nanometer scale. To achieve optimal segmentation results, the image analysis process was broken down into two parts (Fig. 1). The first part involved finding of a region of interest that included a cell nucleus. The second step of the analysis was the segmentation of the nucleus in the region of interest.

The selection of the region of interest was fully automated by reducing image noise by two-dimensional median filtering followed by maximum intensity projection of the whole image stack. The two-dimensional image obtained was segmented using a neighborhood connected threshold region growing filter (NCTRG, ITK toolkit; Kitware, Inc., Clifton Park, NY) integrated into TIKAL. The NCTRG filter is an extension of the standard connected region growing filter using mathematical morphology erosion. The reason for considering neighborhood intensities in the erosion process, instead of only the current pixel intensity, is that small structures are more likely to be segmented. The basic approach of the NCTRG algorithm is to start from a seed region that is considered to be inside the object to be segmented.

For our automated segmentation we used an inverted approach; that is, we segmented regions not belonging to objects (background) and finally inverted the resulting image to obtain the binary nuclei regions. This strategy has several advantages, in particular the selection of a seed point is independent of the actual position of the cell nucleus in the image; that is, selection of the seed point can always be in the left upper corner of the image. Another advantage to segmenting the background is low intensity fluctuations within the background areas resulting in smooth object borders. High reliability of this inverted segmentation approach was crucial for application in a fully automated high-throughput setting.

After obtaining a segmented two-dimensional representation of the whole image area, individual binary cell nuclei were selected and used as template to define regions of interest in each individual image of the three-dimensional stack. The region of interest was then processed by contour preserving and noise reducing three-dimensional anisotropic diffusion filtering[23] followed by NCTRG in three dimensions using the same background segmentation strategy as described above. As a result, we obtain accurately segmented cell nuclei in three-dimensions.

Distance measurements. An automated segmentation of the *Xic* FISH signals was not possible owing to their variable intensity and size. Manual selection and segmentation of the *Xic* signal was therefore performed after segmentation of cell nuclei. This also allowed detection and correction of possible segmentation artefacts in the DAPI channel; for example, overlapping nuclei. To estimate the distance of the *Xist–Xic* region to the periphery and the inter *Xist–Xic* distance, we implemented a new module in TIKAL. This module is capable of finding the closest distance of two segmented objects in different channels. For this purpose the *Xic* signal was automatically pre-processed by reducing noise using two-dimensional median filtering followed by three-dimensional anisotropic diffusion filtering. Segmentation was obtained using NCTRG with a seed point in a background region. The segmentation results were manually cross validated against the original raw *Xist–Xic* data and if necessary corrected to avoid false segmentation. After this data validation, the centre of mass of each segmented signal was obtained automatically. The shortest Euclidian distances of the centre of mass to the closest segmented nuclear peripheral voxel were calculated. The inter *Xic* distance was obtained by measuring the three-dimensional Euclidean distance of the two segmented *Xist–Xic* centres of mass within the cell nucleus.

Statistical analysis, simulation and plots. Statistical analyses were performed in R (http://www.r-project.org/). For coherence, the distributions were compared with two non-parametric tests, namely Wilcoxon and Kolmogorov–Smirnov[24,25]. Both tests showed similar results for the analysis. Cutoff threshold for similar distribution was the 95% quantile.

Simulations of random data points and quantile–quantile plot generation were performed in R (http://www.r-project.org/) and are described in more detail below. Live cell-line plots and bar plots were generated with Sigmaplot.

For data simulation, random points with equal density distribution in a unit sphere were generated. For this purpose the volumes of all segmented nuclei were combined and the median volume calculated, which resulted in an approximation of a hypothetical cell nucleus with a radius of 7.2 μm. To simulate the *Xic* distance from the nuclear periphery, 1,000 random spots within this sphere were generated by individually selecting the *x*, *y* and *z*, coordinates from a random uniform distribution number generator provided by the R program. Finally, the shortest distances to the nuclear periphery were calculated by correlating the obtained three-dimensional points to the previously determined simulated nuclear radius. Similar procedures were chosen for the simulation of distances between two hypothetical *Xic* signals. Individual uniformly distributed *x*, *y* and *z* coordinates (2 × 1,000) were generated followed by calculation of the Euclidean distance between two three-dimensional coordinates resulting in 1,000 simulated inter-*Xic* distances.

The quantile-quantile plot is a graphical technique for determining whether two data sets come from populations with a common distribution. The method plots the quantiles of the first data set against the quantiles of the second data set. If the two sets come from a population with the same distribution, the points should fall approximately on a line with a slope of one. The larger the deviation from this reference line, the greater the evidence that the two data sets originated from populations with different distributions[26].

Note: Supplementary Information is available on the Nature Cell Biology website.

ACKNOWLEDGMENTS

We would like to thank A. Belmont, D. Spector and N. Mise for helpful comments on the manuscript and P. Le Baccon for support with image analysis. This project was supported by a Human Frontier Science Program (HFSP) research grant to E.H. and R.E. R.E. also acknowledges support on multi-dimensional image acquisition from Leica Microsystems CMS GmbH, Mannheim, Germany. Support to E.H. was also provided by the Schlumberger Foundation, the Centre National de la Recherche Scientifiques (CNRS) and the Curie Institute (Program Incitatif et Collaboratif). E.H. and P.A. are also supported by the EU Network of Excellence (Epigenome).

COMPETING FINANCIAL INTERESTS

The authors declare that they have no competing financial interests.

Published online at http://www.nature.com/naturecellbiology/
Reprints and permissions information is available online at http://npg.nature.com/reprintsandpermissions/

1. Rastan, S. Non-random X-chromosome inactivation in mouse X-autosome translocation embryos — location of the inactivation centre. *J. Embryol. Exp. Morphol.* **78,** 1–22 (1983).
2. Rastan, S. & Robertson, E. J. X-chromosome deletions in embryo-derived (EK) cell lines associated with lack of X-chromosome inactivation. *J. Embryol. Exp. Morphol.* **90,** 379–388 (1985).
3. Boumil, R. M. & Lee, J. T. Forty years of decoding the silence in X-chromosome inactivation. *Hum. Mol. Genet.* **10,** 2225–2232 (2001).
4. Clerc, P. & Avner, P. Multiple elements within the *Xic* regulate random X inactivation in mice. *Semin. Cell Dev. Biol.* **14,** 85–92 (2003).
5. Clerc, P. & Avner, P. Role of the region 3 to *Xist* exon 6 in the counting process of X-chromosome inactivation. *Nature Genet.* **19,** 249–253 (1998).
6. Morey, C. *et al.* The region 3' to *Xist* mediates X chromosome counting and H3 Lys-4 dimethylation within the *Xist* gene. *EMBO J.* **23,** 594–604 (2004).
7. Heard, E., Mongelard, F., Arnaud, D. & Avner, P. *Xist* yeast artificial chromosome transgenes function as X-inactivation centers only in multicopy arrays and not as single copies. *Mol. Cell Biol.* **19,** 3156–3166 (1999).
8. Marahrens, Y. X-inactivation by chromosomal pairing events. *Genes Dev.* **13,** 2624–2632 (1999).
9. Osborne, C. S. *et al.* Active genes dynamically colocalize to shared sites of ongoing transcription. *Nature Genet.* **36,** 1065–1071 (2004).
10. Spilianakis, C. G. *et al.* Interchromosomal associations between alternatively expressed loci. *Nature* **435,** 637–645 (2005).
11. Spector, D. L. The dynamics of chromosome organization and gene regulation. *Annu. Rev. Biochem.* **72,** 573–608 (2003).
12. Taddei, A., Hediger, F., Neumann, F. R. & Gasser, S. M. The function of nuclear architecture: a genetic approach. *Annu. Rev. Genet.* **38,** 305–345 (2004).
13. Chambeyron, S. & Bickmore, W. A. Does looping and clustering in the nucleus regulate gene expression? *Curr. Opin. Cell Biol.* **16,** 256–262 (2004).
14. Comings, D. E. The rationale for an ordered arrangement of chromatin in the interphase nucleus. *Am. J. Hum. Genet.* (1968).
15. Okamoto, I. *et al.* Evidence for *de novo* imprinted X-chromosome inactivation independent of meiotic inactivation in mice. *Nature* **438,** 369–373 (2005).
16. Morey, C., Arnaud, D., Avner, P. & Clerc, P. *Tsix*-mediated repression of *Xist* accumulation is not sufficient for normal random X inactivation. *Hum. Mol. Genet.* **10,** 1403–1411 (2001).
17. Navarro, P. *et al. Tsix* transcription across the *Xist* gene alters chromatin conformation without affecting *Xist* transcription: implications for X-chromosome inactivation. *Genes Dev.* **19,** 1474–1484 (2005).
18. Sado, T., Hoki, Y. & Sasaki, H. *Tsix* silences *Xist* through modification of chromatin structure. *Dev. Cell* **9,**159–165 (2005).
19. Stavropoulos, N., Rowntree, R. K. & Lee, J. T. Identification of developmentally specific enhancers for *Tsix* in the regulation of X chromosome inactivation. *Mol. Cell. Biol.* **25,** 2757–2769 (2005).
20. LaSalle, J. M. & Lalande, M. Homologous association of oppositely imprinted chromosomal domains. *Science* **272,** 725–728 (1996).
21. Rougeulle, C. *et al.* Differential histone H3 Lys-9 and Lys-27 methylation profiles on the X chromosome. *Mol. Cell. Biol.* **24,** 5475–5484 (2004).
22. Bacher, C. P. *et al.* 4-D single particle tracking of synthetic and proteinaceous microspheres reveals preferential movement of nuclear particles along chromatin — poor tracks. *BMC Cell Biol.* **5,** 45 (2004).
23. Tvarusko, W. *et al.* Time-resolved analysis and visualization of dynamic processes in living cells. *Proc. Natl Acad. Sci. USA* **96,** 7950–7955 (1999).
24. Hollander, M. & Wolfe, D. A. in *Nonparametric statistical inference* 27–33 (John Wiley & Sons, New York, 1973).
25. Conover, W. J. in *Practical nonparametric statistics* (ed. Wiley, B.) 295–301 & 309–314 (John Wiley & Sons, New York, 1971).
26. Becker, R. A., Chambers, J. M. & Wilks, A. R. *The New S Language* (Wadsworth & Brooks/Cole, 1988).
27. Penny, G. *et al.* Requirement for *Xist* in X chromosome inactivation. *Nature* **379,** 131–137 (1996).

CORRIGENDUM

Owing to an error, reference 26 was misplaced on page 174 of the article by K. Muthumani *et al.* (**8,** 170–179; 2005). The corrected text should read as follows:

The role of PARP-1 in regulating NF-κB suppression seems to be entirely structural and not associated with its enzymatic properties, as DPQ (a nicotinic acid analogue) and a PARP-1 enzymatic inhibitor, did not significantly repress TNF-α induced NF-κB transcription[26,28].

Reference 28 was cited incorrectly in the reference list. The correct citation is as follows:

28. Hassa, P. O. *et al.* Transcriptional coactivation of nuclear factor-κB-dependent gene expression by p300 is regulated by poly(ADP)-ribose polymerase-1. *J. Biol. Chem.* **278,** 45145–45153 (2003).

The legend for Fig. 2 (**b**–**c**) was incorrect and should state that:
Cells were fixed and stained with an anti-PARP-1 antibody as described in Methods.

These corrections have been made online.

In the article by C. White *et al.* (**7,** 1021–1028; 2005), the error bars shown in the Supplementary Information Fig. S3d were incorrect. Furthermore, the statistical analysis in Figs 4d and S3d was not adequately explained: the error bars represent standard deviations of the mean in three independent experiments for each clone and time point. This has been corrected online.

RETRACTION

Xu, Y., Zhu, K., Hong, G., Wu, W., Baudhuin, L. M., Xiao, Y. & Damron, D. S. Sphingosylphosphorylcholine is a ligand for ovarian cancer G-protein-coupled receptor1. *Nature Cell Biol.* **2,** 261–267 (2000).

We wish to retract this paper due to concerns about data presented in Fig. 1. The principal data in question are the calcium profile data in Fig. 1a. These data were obtained by Dr. Kui Zhu (joint first author), at the time a research fellow in the laboratory of Dr. Yan Xu (senior author), in the Lerner Research Institute of the Cleveland Clinic Foundation. The original data used to compose Fig. 1 cannot be located. The first peaks in the upper and lower panels of Fig. 1a show high homology, although different ligands were used in the two experiments.

An institutional inquiry panel and an investigation panel were formed to determine the possibility of misconduct on the part of Dr. Kui Zhu in two related papers (Kabarowski, J. H. *et al. Science* **293,** 702–705 (2001) and Zhu, K. *et al. J. Biol. Chem.* **276,** 41325–41335 (2001). The committee found Dr. Zhu guilty of data fabrication and scientific misconduct related to these two publications. The very strong similarity of the two traces in Fig. 1 and the lack of original data suggest that similar misconduct occurred by Dr. Zhu in this *Nature Cell Biology* publication.

Owing to the serious concerns about the validity of the data published in the paper, we would like to retract this paper. We deeply regret any inconvenience this publication has caused for others. All authors, apart from Dr. Kui Zhu, have signed this retraction. Dr. Zhu did not return a signature.